Assessment of combined sewer overflows impacts under flooding in coastal cities

Helieh Abbasi, Amin Zeynolabedin and Gholamreza Nabi Bidhendi

ABSTRACT

Wastewater treatment plants (WWTPs) are among the most important infrastructures, especially in coastal cities with a risk of flooding. During intense floods, runoff volume may exceed the capacity of a WWTP causing plant failures. This paper investigates the impacts of flooding on combined sewer overflows (CSOs) in a WWTP in New York City. The impacts of CSOs after flooding are classified into four categories of health, economic, social, and environmental factors. Different factors are defined to evaluate the impacts of CSOs using multi-criteria decision-making of Preference Ranking Organization Method For Enrichment Evaluation and fuzzy technique for order performance by similarity to ideal solution. Since volume and depth were found to be the most significant factors for the CSO impact assessment, the Gridded Surface Subsurface Hydrologic Analysis model was run to compute flood depth and CSO volume under three treatment plant failure scenarios considering the Hurricane Sandy information. Sensitivity analysis revealed that the Total Suspended Solids (TSS), Biochemical Oxygen Demand (BOD), and dissolved oxygen have the highest impacts on CSO. Uncertainty analysis was applied to investigate CSO impact variation. Results show that evaluating the impacts of CSOs in different aspects can help improve the efficiency of flood planning and management during storms.

Key words | coastal flooding, combined sewer overflows, hydrologic modeling, MCDM, wastewater treatment plants

Helieh Abbasi (corresponding author)
Gholamreza Nabi Bidhendi
School of Environmental Engineering,
University of Tehran,
Tehran,
Iran
E-mail: *helieh.abbasi55@gmail.com*;
helieh.abbasi@ut.ac.ir

Amin Zeynolabedin
School of Civil Engineering, College of Engineering,
University of Tehran,
Tehran,
Iran

HIGHLIGHTS

- The impacts of combined sewer overflows (CSOs) after flooding are classified into health, economic, social, and environmental factors.
- Different factors are defined, and consequently, different impacts of CSOs are evaluated using multi-criteria decision-making methods of Preference Ranking Organization Method for Enrichment Evaluation and fuzzy Technique for Order Performance by Similarity to Ideal Solution.
- Floodplain delineation and flood depth are obtained using the Gridded Surface Subsurface Hydrologic Analysis model.
- Under different scenarios, full operation, total failure and partial failure are considered.

doi: 10.2166/wcc.2021.322

INTRODUCTION

Floods as a natural hazard cause significant economic and social costs, and losses of life (Haq *et al.* 2012). One of the infrastructures which can be affected by flooding is combined sewer systems. Combined sewer systems are designed to collect domestic and industrial wastewater and rainwater runoff. During periods of heavy rainfall and flood, the volume of wastewater may exceed the capacity of the treatment plants. Combined sewer systems are designed to be able to overflow and discharge excess wastewater to rivers and other water bodies nearby (UEPA 2001). Hence, many researchers have tried to predict and model flood status in the regions such as Fotovatikhah *et al.* (2018), who presented a comprehensive survey about the application of computational intelligence-based methods in flood management systems. They also introduced the most recent promising approaches with respect to the accuracy and error rate for flood debris forecasting and management. The results showed the model's high efficiency. Burgan & Icaga (2019) applied the Adaptive Hydraulics (AdH) and the Finite Element Surface Water Modeling System models to generate a hydraulic model for flood conditions in the Acarkay basin, Turkey. The results showed that the majority of settled areas would not face flood risk, while agricultural lands in some regions near the banks of streams may experience flood risks. Kaya *et al.* (2019) presented a flood modeling method for rivers having no upstream gauged stations. They predicted upstream hydrograph by the reverse flood routing method. This hydrograph was utilized as an inflow for the HEC-RAS model. They applied the model to Guneysu Basin in Rize Province in the Eastern Black Sea region of Turkey. The comparison of observed data with the produced flood map showed the model's capability. Al-Ani & Al-Obaidi (2019) used a multiple linear regression model (MLRM) and artificial neural network (ANN) for sewer sediment accumulation calculation in Baghdad city, Iraq. The results showed that the MLRM is acceptable, with an R^2 value of 89.55%. The ANN model was found to be practical with an R^2 value of 82.3%. They also applied sensitivity analysis which showed that the flow is the most influential parameter on the depth of sediment deposition. Keum *et al.* (2020) developed a classification-based real-time flood prediction model for urban areas by combining a numerical analysis model based on a hydraulic theory with a machine learning model. The results were compared with a verified two-dimensional model, which indicated that the goodness of fit of the developed model was 85%. The model showed its capability in predicting floods for risk management. Mirra *et al.* (2020) used the oxygen uptake rate (OUR) to show its applicability for the management of onsite wastewater treatment plants (WWTPs). The results proved that when there is no wastewater generation in the household, the OUR in the reactor is very low, 0.0007 to 0.0015 mg/l s, and thus does not require a high oxygen supply. These results, if verified with field experiments, will enable the optimization of the energy use during onsite WWTP operation. Also, other researchers tried to develop prediction methods, such as Wu & Chau (2013), Taormina & Chau (2015), and Mosavi *et al.* (2018).

Due to special situations, coastal cities and their infrastructures in terms of energy, transportation, water, and wastewater are vulnerable due to storm surges, hurricanes, and combined coastal and inland flooding (De Almeida & Mostafavi 2016; Zeynolabedin *et al.* 2020). As an example, Hurricane Sandy was the largest storm to hit the northeast USA in recorded history, killing 159, knocking out power to millions, and causing $70 billion in damage in eight states (Kenward *et al.* 2013). Six months after Sandy, data from the eight hardest-hit states showed that 11 billion gallons of untreated and partially treated sewage flowed into rivers, bays, canals, and in some cases, city streets, largely as a result of record storm-surge flooding that swamped the region's major sewage treatment facilities. The vast majority of that sewage flowed into the waters of New York City (NYC) and northern New Jersey in the days and weeks during and after the storm (Kenward *et al.* 2013).

Combined sewer overflows (CSOs) contain stormwater and untreated human and industrial waste, toxic materials, and debris, so they are considered to be major water pollution in different aspects (Karamouz *et al.* 2015). CSOs are a shock loading to the environment that could cause large amounts of pollutants to enter water bodies including rivers and harbors. They are considered a threat to human and aquatic life (Gandhi 2013). According to the United Environmental Protection Agency (UEPA 2017), approximately 772 cities in the USA

face this problem. A large amount of CSOs spread the pollutants in aquatic environments, so there will be a high tangible or intangible cost involved to get rid of pollution and restore the water quality (Semadeni-Davies *et al.* 2008). The intensity of the stormwater/flood event affects the concentrations of CSOs' pollutants (UEPA 2004). The CSOs' discharge, volume, and duration are important in the context of human health and environmental impacts. These impacts are also dependent on antecedent moisture conditions, groundwater levels, and land use which determine the amount of rainfall infiltration and runoff (UEPA 2013). To quantify CSO impacts, different methods and techniques are used by researchers. For instance, Schroeder *et al.* (2011) analyzed CSO datasets from four catchments of Berlin's combined sewer system in Germany. A comparison of rainfall characteristics (e.g. duration, maximum hourly intensity, and total depth) with CSO volumes showed that total rainfall depth was the best determinant of CSO occurrence. Friedrich & Kretzinger (2012) investigated the vulnerability of wastewater collection and disposal infrastructure such as pipelines and manholes, pumping stations, and wastewater treatment plants caused by sea level rise (SLR). They identified the infrastructural elements within the wastewater system that are most vulnerable to SLR. Hummel *et al.* (2018) mentioned that across the USA, 394 wastewater treatment plants, serving over 31 million people, were exposed to flooding and CSOs. Bae (2020) investigated the effects of CSOs on the river's water quality throughout three preliminary field tests and three main ones in South Korea. The results indicated that CSOs did not affect water quality on the mainstream since their concentration did not significantly change during rainfall events, although the water quality of tributaries has rapidly deteriorated due to the influence of the CSOs during rainfall events.

Generally, previous studies concentrated on a specific aspect of CSOs, ignoring other impacts. Also, most studies lack the uncertainty analysis of CSOs which is an important subject. In this study, the aforementioned gaps are covered by evaluating the impacts of CSOs on different aspects such as economic, social, environmental, and health by applying the multi-criteria decision-making (MCDM) method. An uncertainty analysis is done to investigate the uncertain nature of CSOs. Also, a distributed hydrologic model named GSSHA (Gridded Surface Subsurface Hydrologic Analysis) is used to estimate the volume of runoff and depth of flooding in different parts of the case study. In the following, the methodology is explained in detail, and the corresponding results are delivered and discussed.

METHODOLOGY

In this study, the impacts of CSOs on different aspects such as economic, social, environmental, and health are investigated in the Coney Island treatment plant which is one of the NYC's 14 treatment plants. To assess the impacts of CSOs, four criteria and 22 sub-criteria are selected. By applying the analytic hierarchy process (AHP) method, a weight is assigned to each sub-criterion in order to consider their importance. Then, for quantifying the impact of CSOs, two different MCDM methods, namely fuzzy Technique for Order Performance by Similarity to Ideal Solution (fuzzy TOPSIS) (Hwang & Yoon 1981) and Preference Ranking Organization Method for Enrichment Evaluation (PROMETHEE) (Morais & De Almeida 2007), are employed. Based on the result of MCDM methods and by considering Superstorm Sandy data, the flood depth and runoff volume are obtained for Coney Island WWTP located in NYC by running a distributed hydrologic model named GSSHA (Downer & Ogden 2004). In the end, the CSO's volume is calculated. The flowchart of methodology is delivered in Figure 1.

The methodology is summarized in five main steps delivered in the following:

(1) Dividing CSO evaluation into four main criteria and corresponding sub-criteria,
(2) Weighting sub-criteria by the AHP method,
(3) Quantifying CSO impact using PROMETHEE and fuzzy TOPSIS,
(4) Identifying critical sub-criteria and their variation by running sensitivity and uncertainty analysis, and
(5) Running the GSSHA model for estimating the volume of runoff, depth of inundation in a WWTP, and the volume of CSO.

In the following, the methodology is explained based on the aforementioned steps.

Identifying criteria and sub-criteria (Step 1)

CSOs can result in high concentrations of microbial pathogens, solids, debris, and toxic pollutants. Also, CSOs could

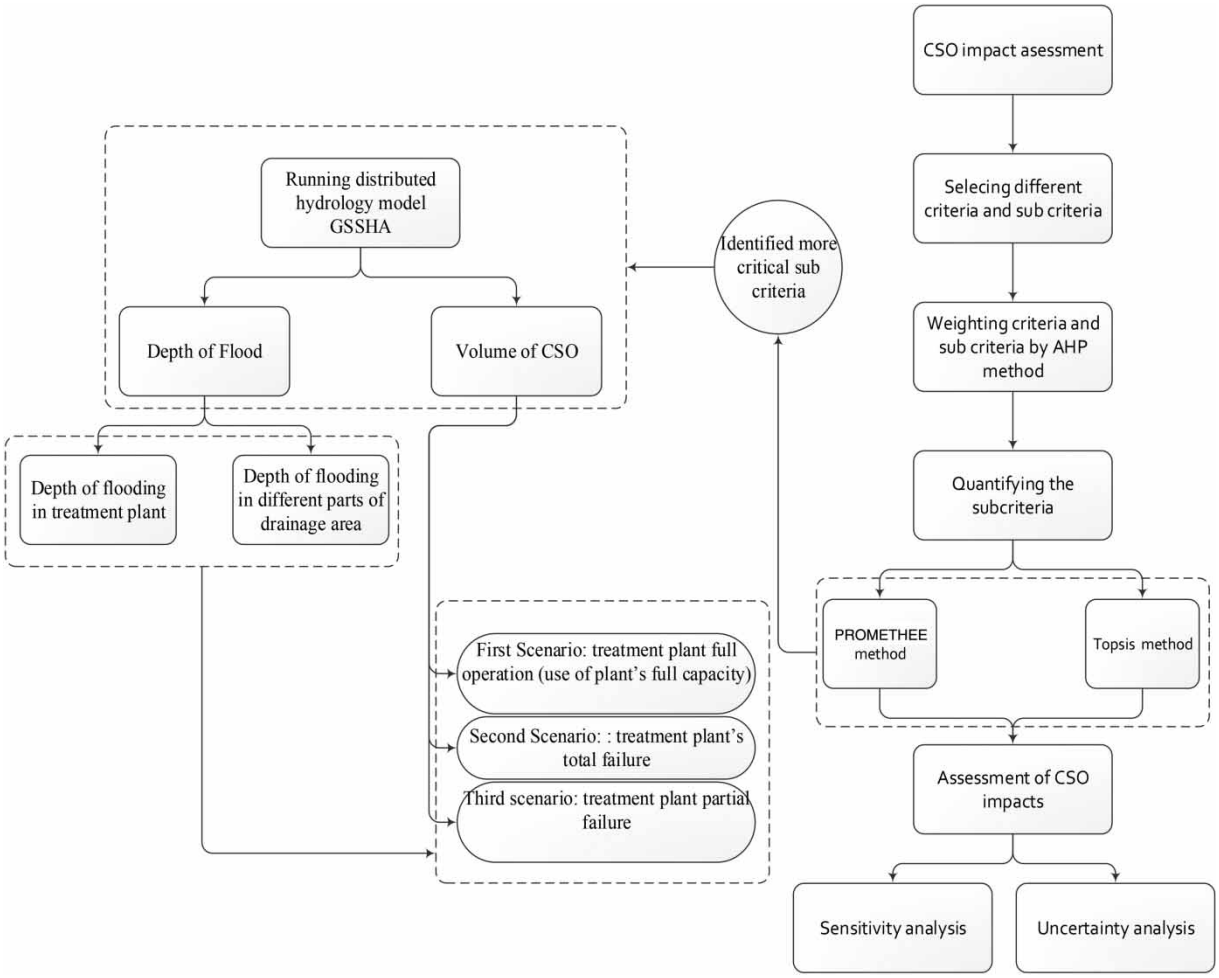

Figure 1 | Flowchart of methodology.

result in severe oxygen deficits that cause water quality concerns by putting stress on public health and aquatic life (House *et al.* 1993; Walsh *et al.* 2005; Holeton *et al.* 2011; Passerat *et al.* 2011; Madoux-Humery *et al.* 2013). The impacts of CSOs can be categorized as short-term and long-term. The short-term impacts appear immediately after a storm. They are due to dissolved contaminants, bacteria, and viruses causing the death of fishes and aquatic life (Boët *et al.* 1994; Kenward *et al.* 2013). Long-term impacts such as oxygen concentrations and ecological damage cause environmental changes slowly over time and affect organisms over generations (Harremoes 1982). In this study, different impacts of CSOs are classified into four main criteria, public health, environmental, economic, and social, with 22 sub-criteria, as summarized in Table 1.

Weighting the sub-criteria (Step 2)

In order to quantify the impact of CSOs, it is necessary to determine the relative importance of each criterion and sub-criterion. For this purpose, an online questionnaire survey based on the pairwise comparison is designed and distributed among professors, Ph.D. students, and engineers familiar with CSOs. According to the survey's results and applying the AHP method, each criterion and sub-criterion is ranked and assigned a weight showing its importance. It results in related weights of criteria using pairwise comparisons between the sub-criteria by using a multi-level hierarchical structure of factors. In the AHP method proposed by Saaty (1977), the pairwise comparisons are considered to be adequately consistent if the corresponding consistency ratio (CR) is less

Table 1 | Criteria and sub-criteria identified for the evaluation of CSOs' impacts

Criteria		Sub-criteria	Label	Units
Human health impacts (A)		Biological active chemicals (bacteria, virus, etc.)	A1	colonies/100 mL
		Toxics (metals and synaptic organic chemicals)	A2	μg/l
		Microbiological pathogens	A3	colonies/100 mL
Environmental impacts (B)	Quantity (B1)	Volume	B11	m^3 and gallon
		Depth	B12	m
		Discharge	B13	m^3/d and gallon/d
	Quality (B2)	Dissolved oxygen (DO)	B21	Ppm
		Sediments and total suspended solids	B22	mg/l
		Water turbidity and water odor	B23	NTU
		Algal growth	B24	%
		Temperature	B25	°C
		Nutrients	B26	mg/l
		pH	B27	–
		Hardness	B28	%
		BOD	B29	mg/l
Social impacts (C)		Changing the value of property	C1	%
		Recreation and tourist (swimming, kayak ring, etc.)	C2	%
		Traffic development caused by flooded street	C3	%
Economic impacts (D)		Cost of collecting contaminant and floatables	D1	%
		Cost of beach closing (fishing, delay in ship placement, …)	D2	%
		Real estate market value	D3	%
		Movement of ships	D4	%

than 10% (Saaty 1977) (Equation (1)):

$$\mathrm{CR} = \frac{\frac{\lambda_{\max} - n}{(n-1)}}{\mathrm{RI}} \tag{1}$$

where $\lambda_{\max}$ is the maximal eigenvalue, n is the dimension of the matrix, and RI is a random index for $n \times n$ matrix.

Quantifying CSO impact (Step 3)

In order to quantify the impact of CSOs, fuzzy TOPSIS (Zadeh 1996; Hwang & Yoon 1981) and PROMETHEE (Vincke & Brans 1985) methods are applied which are explained in the following.

PROMETHEE method

The sub-criteria introduced in Table 1 have different orders and units. To apply the PROMETHEE method, standardization is needed. Hence, three different values (as alternatives) for each sub-criterion including maximum, minimum, and actual value are collected. For a specified sub-criterion, the arithmetic difference between evaluations of any two pairs (Equation (2)) is used for scaling down values between zero and one (standardization).

$$\bar{c}_n(v_i, v_j) = \frac{b_n(v_i, v_j) - b_{n,\min}}{b_{n,\max} - b_{n,\min}} \quad \forall\ n \in N_R \tag{2}$$

where i and j signify the ith and jth alternatives, respectively, v represents the actual value of sub-criterion, $b_n(v_i, v_j)$, corresponding to the nth sub-criterion, is calculated as $v_i - v_j$, $b_{n,\min}$ and $b_{n,\max}$ represent the minimum and maximum values of differences for the nth sub-criterion, respectively, and N_R is the total number of sub-criteria considered for quantifying CSO impacts. Based on the PROMETHEE method, the metric to quantify the CSO impacts for jth alternative (CSO_j) is calculated as follows (Equation (3)):

$$\mathrm{CSO}_j = \left(\sum \left(\frac{1}{m-1} \times \sum_j^n \left(\bar{c}_n(v_i, v_j) - \bar{c}_n(v_j, v_i) \right) \right) \times w_n + 2 \right) \times 50 \tag{3}$$

where w_n represents the weights corresponding to the nth CSO sub-criteria, and m is the total number of alternatives.

Fuzzy TOPSIS method

The main purpose of the fuzzy TOPSIS method is to estimate the closeness of alternatives to ideal solutions in the decision-making process. To evaluate the chance of an alternative, the closeness coefficient will be estimated during the process; the higher the value of the closeness coefficient, the more closeness to ideal solutions. The main steps of the proposed fuzzy TOPSIS method can be described as follows:

1. Determination of decision matrix (Equation (4)):

$$X = \begin{bmatrix} x_{11} & x_{12} & \dots & x_{1n} \\ x_{21} & x_{22} & \dots & x_{2n} \\ \dots & \dots & \dots & \dots \\ x_{m1} & x_{m2} & \dots & x_{mn} \end{bmatrix} \quad (4)$$

2. Normalizing (Equation (5)):

$$r_{ij} = \frac{x_{ij}}{\sqrt{\sum_{i=1}^{m} x_{ij}^2}} \quad (5)$$

3. Determination of the weighted normalized decision matrix using the weights obtained from the AHP method output (Equation (6)):

$$t_{ij} = r_{ij} \times w_j \quad (6)$$

4. Calculation of the distance of each alternative from fuzzy positive (t_i^+) and fuzzy negative (t_i^-) ideal solutions (Equation (7)):

$$d_i^+ = \sqrt{\sum_{j=1}^{n} \frac{1}{3} \times (t_{ij} - t_i^+)^2}, \quad d_i^- = \sqrt{\sum_{j=1}^{n} \frac{1}{3} \times (t_i^- - t_{ij})^2} \quad (7)$$

5. Calculations of closeness coefficient index (Equation (8)):

$$C_i = \frac{d_i^-}{d_i^- + d_i^+} \quad (8)$$

Conservation scales are applied to transform the linguistic terms into fuzzy numbers. Table 2 illustrates linguistic variables and related triangular fuzzy numbers to assess the criteria weights importance. According to this table, we have seven different importance levels, and each sub-criterion has a specific importance level. As an example, IM4 indicates equal importance with negative or positive triangle fuzzy numbers.

Table 2 | Linguistic variables and related triangular fuzzy numbers

Alternative assessment	Importance level	Triangle fuzzy numbers (negative)	Triangle fuzzy numbers (positive)
Much less important	IM1	(0.9,1,1)	(0,0,0.1)
Less important	IM2	(0.7,0.9,1)	(0,0.1,0.3)
Relatively less important	IM3	(0.5,0.7,0.9)	(0.1,0.3,0.5)
Equal	IM4	(0.3,0.5,0.7)	(0.3,0.5,0.7)
Relatively important	IM5	(0.1,0.3,0.5)	(0.5,0.7,0.9)
Important	IM6	(0,0.1,0.3)	(0.7,0.9,1)
Very important	IM7	(0,0,0.1)	(0.9,1,1)

Evaluating the impact of sub-criteria on CSO impact (Step 4)

Sensitivity analysis

In this study, six factors are considered for sensitivity analysis to investigate how they affect the CSO impact variation. For this purpose, two sensitivity analysis methods are applied namely OAT (one factor at a time) and GSA (global sensitivity analysis). In the OAT method, the changes in model outputs are only related to a specific parameter. It does not consider the effects of varying two or more parameters simultaneously which is the limit of this method. To apply OAT, first, all parameters are set at their default values and the model is simulated. Next, each parameter individually is varied between its maximum and minimum values, while all others are held at their default values. In the end, the percentage change in each model output is calculated to determine which parameters cause the greatest and lowest variations in model outputs.

Beside the OAT, the GSA method is applied to obtain an understanding of higher-order effects and consider further combination changes in parameters. For applying GSA, Sobol's method (Sobol 2001) is used which enables first-, second-, and higher-order effects to be distinguished through

the calculation of sensitivity indices for each parameter or parameter pair. It requires fewer model evaluations and provides more robust sensitivity rankings with better model performance than other GSA methods such as analysis of variance (Tang *et al.* 2007). The total variance (D) of model outputs is computed as follows with the assumption of parameters independence (Tang *et al.* 2007):

$$D = \sum_{i} D_i + \sum_{i<j} D_{ij} + \sum_{i<j<k} D_{ijk} + \ldots + D_{12\ldots p} \tag{9}$$

where p is the total number of parameters, D_i is the output variance resulting from the ith parameter, and D_{ij} is the output variance resulting from the interaction between the ith and jth parameters.

First-, second-, and total-order sensitivity indices S_i, S_{ij}, and S_{Ti} are calculated by the following equations:

$$S_i = \frac{D_i}{D} \tag{10}$$

$$S_{ij} = \frac{D_{ij}}{D} \tag{11}$$

$$S_{Ti} = 1 - \frac{D_{\tilde{i}}}{D} \tag{12}$$

where S_i is the first-order sensitivity index which represents the percentage contribution of the ith parameter, S_{ij} is the second-order sensitivity index representing the interaction between the ith and jth parameters to total variance, S_{Ti} is the total-order index which represents the percentage contribution related to the ith parameter, including the interactions of any order, and $D_{\tilde{i}}$ is the output variance resulting from all parameters except the ith parameter.

It should be noted that higher first-order sensitivity index values indicate a parameter that provides a large contribution to output variance, while lower values indicate a parameter whose interactions result in significant output variance but individually has little effect.

Uncertainty analysis

According to the nature of sub-criteria defined for the evaluation of CSO impacts, there are uncertainties associated with the selected and estimated values. In this study, a new code is developed in MATLAB software based on the Monte Carlo simulation to apply uncertainty analysis. The Monte Carlo simulation is a numerical procedure to reproduce random variables that preserve the specified distributional properties (Tung & Yen 2006; Moya *et al.* 2013). In the Monte Carlo simulation, the response of the system of interest is repeatedly measured under various system parameter sets generated from the known or assumed probabilistic distributions. Not all of the sub-criteria could be treated as random numbers; therefore, a number of them are selected for this part of the analysis. The following steps are taken for uncertainty analysis based on the Monte Carlo method:

1. Six sub-criteria in the environmental impact category are selected for uncertainty assessment, i.e. Biochemical Oxygen Demand (BOD) (B29), DO (B21), algal growth (B24), Total Suspended Solids (TSS) (B22), and nutrients (B26). These sub-criteria are also related to each other, and any change in their values will alter the final index noticeably. Therefore, these six factors were selected for uncertainty assessment.
2. For the aforementioned sub-criteria, the proper distribution should be chosen for generating random values for each of the selected sub-criteria. Different distributions such as gev, rician, gamma, nakagami, weibull, uniform, and normal are examined to determine the best distribution function to fit the observed values.
3. For each factor, 200 values were generated based on its distribution, and by utilizing the PROMETHEE approach, the range of variation of CSO impact index is obtained.

Quantifying CSO volume (Step 5)

The evaluation of the CSO volume can be beneficial for monitoring or modeling control strategies. Equation (13) is used for estimating CSOs volume:

$$Q_o = Q_c + Q_d - Q_p \tag{13}$$

where Q_o is the volume of CSO per unit time, Q_c is the volume of runoff obtained from the hydrologic model (GSSHA), Q_d is the volume of average municipal dry-weather wastewater flow per unit time, and Q_p is the capacity of the waste treatment facility.

Flood scenarios

When a flood happens, a treatment plant's structure and its operation are subject to severe challenges that could result in partial or total operational failure. Here, for quantifying CSO volumes in different situations, three scenarios are defined that can be used to quantify the treatment plant response to flooding: (1) full operation of the treatment plant, (2) total failure after flooding, and (3) partial failure.

Flood depth calculation

Evaluating the flood depth can be considered a good indicator in determining if the wastewater treatment plant fails or not. Hence, to obtain the flood depth resulting from the interaction of rainfall and coastal flooding, the GSSHA model is used. The GSSHA model is included in the Watershed Modeling System (WMS). GSSHA is a 2D distributed hydrologic model with the capability of using the Digital Elevation Map and GIS layers such as soil and land use for the illustration of flooded area and inundation depth. This model can combine the rainfall–runoff model for overland flow and coastal flooding simulation models from SLR. The base of the flood inundation simulation model is the equations of continuity and momentum (Horritt & Bates 2001; Toda *et al.* 2005). The surplus rainfall is estimated by the following equation:

$$R_e = P - I_i - I_g \tag{14}$$

where R_e is surplus rainfall, P is precipitation, I_i is the interception, and I_g is the infiltration amount. The study area is divided into different equal-sized grids (30×30), and the flood inundation for each grid is estimated. To estimate the infiltration, the Green-Ampt infiltration equation is used (Maidment 1993). After determining the overland flow, the flow movement direction is estimated. For this aim, the relationship between the overland flows of each grid with its four adjacent grids, including its up, down, right, and left, should be surveyed together. Based on the continuity equation, the variation in the head at a grid located (i, j), $h^{i,j}$, is estimated as follows (Equation (15)):

$$\frac{\mathrm{d}h^{i,j}}{\Delta t} = \frac{Q_{\text{up}} + Q_{\text{down}} + Q_{\text{left}} + Q_{\text{right}}}{\Delta x \Delta y} + \frac{R_e}{\Delta t} \tag{15}$$

where Q_{up}, Q_{down}, Q_{left}, and Q_{right} are flow from the grids. Δx and Δy are the dimension of grids in x and y directions and Δt is the time interval. To determine the flow directions between cells, a momentum equation is used. Manning's formula is used for the estimation of flow regarding the water depth in adjacent cells. The governing equations are given in the following equations:

$$Q_x^{ij} = \pm \frac{d_{i,j}^{\frac{5}{3}}}{n} S_{\text{fx}}^{\frac{1}{2}} \tag{16}$$

$$S_{\text{fx}} = \left| \frac{h^{i-1,j} - h^{i,j}}{\Delta x} \right| = \left| S_0 - \frac{d^{i-1,j} - d^{i,j}}{\Delta x} \right| \tag{17}$$

$$S_0 = \frac{\Delta g}{\Delta x} \tag{18}$$

where n is the Manning's coefficient, S_0 is the bed slope, S_{fx} is the energy grade line slope, $d_{i,j}$ is the depth of water in the cell; Δg is the topographic elevation difference, and Q_x is the flow rate between grid cells in the x direction, whose sign depends on the flow direction. The flow from the sea toward the land at the interface between the coastline and floodplain area is calculated using Manning's formula based on the overland flow and the water head at the seaside (Zheng *et al.* 2008). The water depth at each grid in the next time interval is calculated using the continuity equation (Equation (19)) (Golian *et al.* 2012):

$$\begin{aligned} d_{ij}^{t+1} &= d_{ij}^{t} + \Delta t \left(\frac{Q_{i-1,j}^{t} - Q_{ij}^{t}}{\Delta x \Delta y} + \frac{Q_{i,j-1}^{t} - Q_{ij}^{t}}{\Delta x \Delta y} \right) \\ &= d_{ij}^{t} + \Delta t \left(\frac{Q_{\text{up}}^{t} - Q_{\text{down}}^{t}}{\Delta x \Delta y} + \frac{Q_{\text{left}}^{t} - Q_{\text{right}}^{t}}{\Delta x \Delta y} \right) \end{aligned} \tag{19}$$

where d_{ij}^{t+1} and d_{ij}^{t} correspond to water depth of grid (i,j) at time interval $t+1$ and t, respectively, and Δt is the time interval.

CASE STUDY

Old urban areas with combined sewer systems, especially coastal cities, are subject to the overflow of billion cubic meters of CSOs to the nearby water bodies every year (Karamouz & Abbasi 2016). It is necessary to study the functionality of sewer systems in these areas for extreme conditions such as storms and hurricanes. NYC is the most populated city in the USA with over 8.3 million people (2019 estimation) distributed over 784 km^2. It is located in 40°43′N and 73°56′W at the southern tip of the State of New York. The average annual rainfall and temperature values are 12.1 °C and 1,144 mm, respectively.

NYC is a coastal city that is in danger of hurricanes and tropical cyclones causing storm surges and flooding. Also, SLR and coastal erosion have made much of the NYC coastline vulnerable to flooding (Gornitz *et al.* 2002; Bowman *et al.* 2008). Since the 17th century, several severe hurricanes, storms, and cyclones have affected NYC causing serious damage to critical infrastructures, such as transportation, and energy systems which were inundated and shut down for days (Kenward *et al.* 2013). The characteristics of different hurricanes that occurred in NYC are delivered in Appendix B. Hurricane Sandy, which occurred in 2012, was the largest super storm ever recorded with the speed of 160.9 km/h, the highest peak of water level (3.49 m) and damage amounting to $75 billion. Table 3 indicates data information for the NYC basin in 2012.

After Hurricane Sandy, more than 41 million m^3 (11 billion gallons) of overflows were discharged into the rivers, harbors, and other surrounding water bodies of the USA. From this amount, one-third of 13 million m^3 (3.45 billion gallons) was untreated sewage, and the remaining 28 million m^3 (7.55 billion gallons) was partially treated with just chlorination or filtration (Kenward *et al.* 2013). NYC had a total amount of 20 million m^3 (5.2 billion gallons) of untreated or partially treated sewage overflow after Hurricane Sandy (Kenward *et al.* 2013). Raw sewages generated in NYC combined with stormwater are first collected by the drainage system and then directed to the city's 14 WWTPs. The locations of NYC's 14 WWTPs and their covered areas are shown in Figure 2. Table 4 shows the volume of untreated and partially treated overflow after Hurricane Sandy in all WWTPs in NYC. Also, the location of CSO's outfalls is shown in Appendix C.

Among different treatment plants in NYC, Coney Island has the lowest resiliency and is vulnerable to flooding (Kokoszka 2013). This plant has the highest amount of CSO overflow. Therefore, it is selected as the focus area of this study. During Superstorm Sandy, Coney Island WWTP was inundated and shut down for 2 h in order to minimize damage to the personnel and electrical equipment. The characteristics of Coney Island WWTP are summarized in Appendix D.

Table 3 | Data information for NYC basin in 2012 in monthly time step in the NYC central park station (NOAA 2012; NYC 2012a)

Data (monthly collected)	Minimum	Maximum	Mean	Std. Dev.
Precipitation (mm)	24.38	136.65	81.53	34.54
Wind (km/h)	12.89	19.47	16.8	2.26
Temperature (°C)	2.7	21.66	13.23	−10.57
Turbidity (NTU)	0.5	9.5	1	0.25
pH	6.7	9.2	7.2	0.1
Nitrate (mg/l)	0.1	0.23	0.17	0.03
Hardness (mg/l $CaCo_3$)	17	21	19	6.85

RESULTS

Weighting the sub-criteria

The estimated weights for sub-criteria based on AHP pairwise comparison from the questionnaire outputs are shown in Table 5. These weights are normalized, so that the summation of the weights for each criterion would be one. Also, the corresponding CR is 3% (less than 10%) which is considered acceptable. Based on Table 5, it can be concluded that environmental impacts are the most important aspect of CSOs based on experts' opinions.

Assessment of CSO impacts

The CSO impact is assessed by two different methods. Based on the PROMETHEE method developed in MATLAB, an average value of 0.475 was obtained for the CSO impact, which indicates an average condition for the CSO impacts followed by Sandy. According to the fuzzy TOPSIS index,

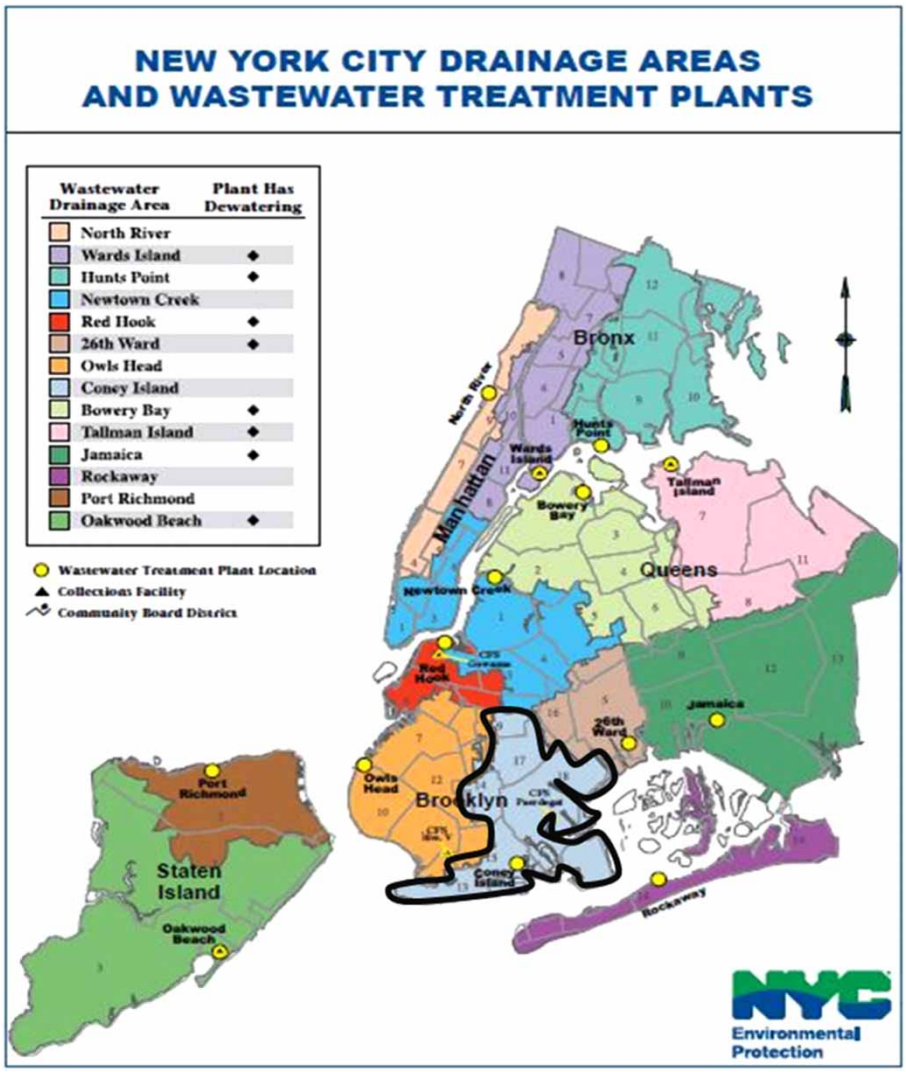

Figure 2 | Location of different wastewater treatment plants of NYC and the covered area (NYC 2012).

Table 4 | Volume of overflow in different treatment plants after Hurricane Sandy (Kenward *et al.* 2013)

Name	Sum of untreated overflow and partially treated (million m^3)	Name	Sum of untreated overflow and partially treated (million m^3)
Coney Island	1.9	Bay Park	8.8
Oakwood Beach	0.9	Yonkers Joint	5
Rockaway	0.8	Port Richmond	0.2
Hunts Point	0.6	Stony Point	0.4
Newtown Creek	0.6	Wards Island	
26th Ward	0.5	Tallman Island	
North River	0.3	Other (31 pump stations)	
Owls Head	0.3	Total New York city overflow	~20 million m^3 (5.2 billion gallons)

Table 5 | Estimated weights of different sub-criteria

Sub-criteria		Label	Weight
Biological active chemicals (bacteria, virus, etc.)	$A = 0.300$	A1	0.323
Toxics (metals and synaptic organic chemicals)		A2	0.354
Microbiological pathogens		A3	0.323
Volume	$B = 0.333$	B11	0.345
Depth		B12	0.332
Discharge		B13	0.323
Dissolved oxygen (DO)		B21	0.202
Sediments and total suspended solid		B22	0.196
Water turbidity and water odor		B23	0.054
Algal growth		B24	0.101
Temperature		B25	0.041
Nutrients		B26	0.101
pH		B27	0.051
Hardness		B28	0.053
BOD		B29	0.201
Changing the value of property	$C = 0.134$	C1	0.333
Recreation and tourist (swimming, kayak ring, etc.)		C2	0.467
Traffic development caused by flooded street		C3	0.2
Cost of collecting contaminant and floatables	$D = 0.233$	D1	0.333
Cost of beach closing (fishing, delay in ship placement …)		D2	0.250
Real estate market value		D3	0.125
Difficulty moving ships		D4	0.292

the relative closeness to the ideal solutions C_i (TOPSIS index) is determined, and the results are delivered in Table 6. Based on the results, depth and volume sub-criteria have the highest rank while temperature has the lowest.

Sensitivity analysis

OAT sensitivity results show that the CSO impact index will be varied between 0.48 and 0.54 due to changes in input variables (Figure 3). The detailed results indicate that between water quality parameters, BOD, dissolved oxygen (DO), and TSS have the highest impact on CSO, while algae and nutrient have the lowest impact (Figure 4). The histogram of the CSO impact index is presented in Figure 5.

On the other hand, the GSA sensitivity analysis shows that TSS, BOD, and DO have the highest impact on CSO, respectively, while nutrients and algae have the lowest impact. The results are summarized in Table 7.

Uncertainty analysis

Five sub-criteria of BOD, DO, TSS, nutrients, and algal growth are selected for uncertainty analysis due to their uncertain nature. In this regard, 200 random numbers for each factor are generated using different distributions between their minimum and maximum values. The results show a relatively wide range of 0.15–0.55 (Figure 6(a)). For estimating the probability density function (PDF) and cumulative distribution function, a non-parametric method called Kernel density estimation is used. Figure 6(b) shows the values for the histogram of the CSO impact index and empirical PDF fitted to the data using Kernel.

Based on the 200 generated values of CSO impacts, generalized extreme value (gev) distribution is the most appropriate fitted distribution among other distributions mentioned in the Methodology. The PDF of fitted distribution functions is shown in Figure 7.

Therefore, at times of severe flooding, there are more uncertainties associated with other elements of CSOs generated such as runoff volume into dependencies of the different parts of WWTP as far as their failure is concerned and its water quality characteristics.

Floodplain delineation

The result of the delineated floodplain by the hydrologic model (WMS-GSSHA) during Superstorm Sandy is shown in Figure 8. Superstorm Sandy was an event that lasted for 2 days. This period was considered in floodplain mapping, which is based on the idea that, during the 2-day event, the flood inundation changes with time. The most critical inundation depth is estimated at 3.78 m (12.40 ft) in the whole study area. Figure 8 shows the most critical inundation depth in different parts of the area for each cell. In the next step, the location of the treatment plant is specified and flood depth is observed in all of the cells of WWTP's location. The critical depth of flooded inundation in the treatment plant was observed as 3.23 m (10.6 ft) during Superstorm Sandy.

Table 6 | Evaluation of Fuzzy TOPSIS for rating different sub-criteria

Criteria		Sub-criteria	importance level	Min value	Actual value	Max value	di+	di_	ci
Human health impacts		Biological Active chemicals (bacteria, virus..)		70	640	1000	0.8507	0.1876	0.181
		Toxics (metals and synaptic organic chemicals)		50	379	2140	0.8744	0.2026	0.188
		Microbiological Pathogens		80	456	2300	0.8800	0.1865	0.175
Environmental impacts	quantity	volume		0	663	883	0.8266	0.2281	0.216
		depth		0	3.23	3.78	0.8467	0.1980	0.190
		discharge		0	332	442	0.8822	0.1513	0.146
	quality	Dissolved Oxygen (DO)		1.8	3	12.7	0.8889	0.1518	0.146
		Sediments and total suspended solid		1	180	4420	0.9468	0.0935	0.090
		Water turbidity and water odour		1.2	3.1	6.5	0.9843	0.0185	0.018
		Alga growth	IM5	0.5	0.7	0.9	0.9545	0.0468	0.047
		Temperature		0.9	11.3	24.4	0.9905	0.0121	0.012
		Nutrients		0.05	50	66.4	0.9535	0.0583	0.058
		pH		6.62	7.27	7.52	0.9804	0.0196	0.020
		hardness	IM5	0.5	0.7	0.9	0.9747	0.0260	0.026
		BOD		3.9	150	696	0.9028	0.1507	0.143
Social impacts		Changing the value of property	IM3	0.5	0.7	0.9	0.8651	0.1923	0.182
		Recreation and tourist (swimming, kayak ring,..)	IM6	0	0.1	0.3	0.8519	0.1940	0.185
		Traffic development caused by flooded street	IM6	0.7	0.9	1	0.8539	0.1911	0.183
Economic impacts		Cost of collecting contaminant and floatable	IM1	0	0	0.1	0.9256	0.1415	0.133
		Cost of beach closing (fishing, delay in ship placement…)	IM2	0	0.1	0.3	0.8808	0.1744	0.165
		Real Estate market value	IM4	0.3	0.5	0.7	0.8904	0.1160	0.115
		Difficulty moving ships	IM1	0	0	0.1	0.9237	0.1455	0.136

The runoff volume obtained from the GSSHA hydrologic model is 10.5 MCM (2.385 billion gallons) for the entire area. Considering the Coney Island WWTP drainage area (32% of the entire area), the runoff estimation is about 32% of the whole volume, i.e., 3.3 MCM (763 million gallons). According to the information obtained from the official NYC website (NYC 2012b), the water consumption in NYC is estimated at 0.476 m^3/day (125.8 gallons/day) for each person. Considering

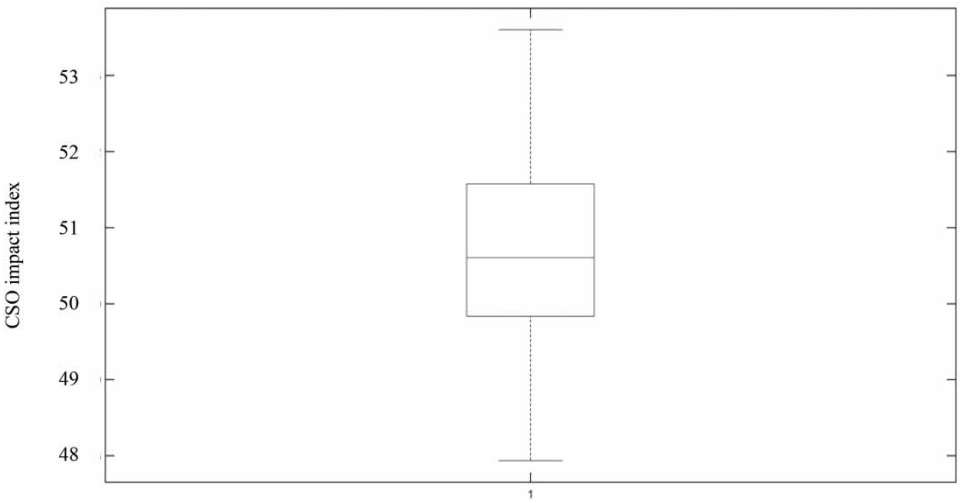

Figure 3 | CSO impact index variation due to sensitivity analysis.

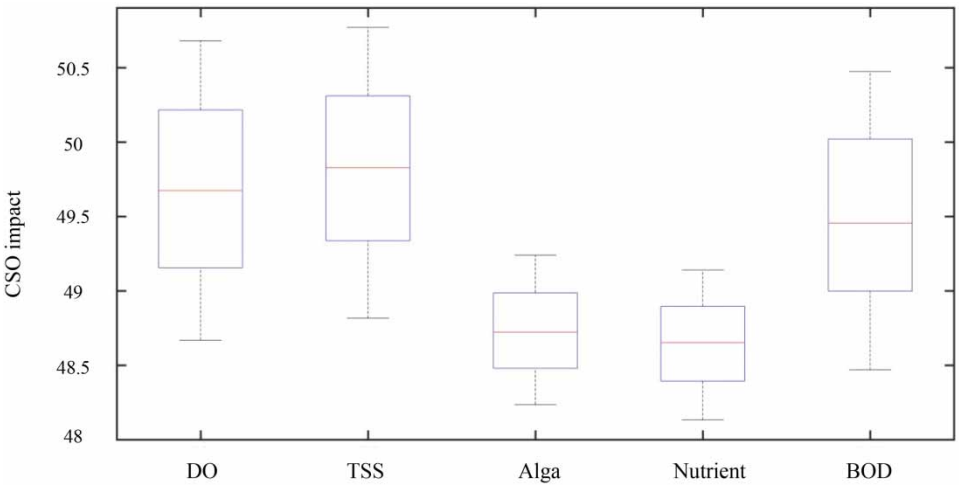

Figure 4 | Impact of water quality parameters in CSO impact index variation.

this amount, approximately 80% of water is converted into wastewater; therefore, the wastewater rate is estimated at 0.380 m^3/person (100.56 gallons/person). Considering the population in the drainage area of Coney Island WWTP (596,326 people), the produced volume of wastewater is 0.28 MCM (60 million gallons/day in this area; hence, 0.52 MCM for 2 days of Sandy) during the modeling time period.

Flood scenarios

According to the MCDM results, environmental impacts are more critical among the CSOs' impact criteria. Based on the WWTP operational state, three scenarios of full operation, total and partial failures are defined. The main assumption is that the extreme event and runoff volume are the same for all scenarios. Since the extreme event dominated the second scenario, in reality, it is assumed that some structural and nonstructural measures are done to mitigate flooding impacts. Depending on the applied measures, in different situations, different scenarios can occur. For the first scenario, the WWTP works well without any disruption. The second one refers to a situation in which the main components of WWTP fail due to flood inundation leading to total failure of the system. In the third scenario, some parts of WWTP are being flooded and then fail. It is assumed

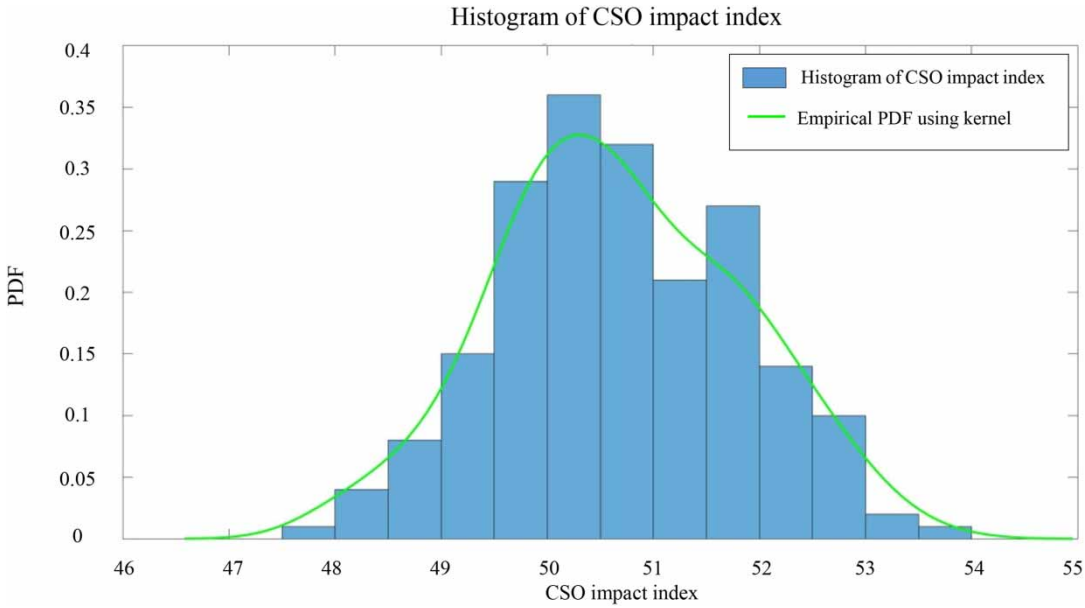

Figure 5 | Histogram of CSO impact index.

Table 7 | CSO volume for different flood scenarios

Parameter	First-order GSA coefficient	GSA rank	OAT rank	OAT coefficient
DO	0.000801184	3	2	1.98729
TSS	0.004704881	1	3	1.95079
Algae	0.0001037	5	4	1.00338
Nutrient	0.000504802	4	5	1.0028
BOD	0.004053441	2	1	1.99333

that WWTP continues its performance with the parts that are not flooded. Since different parts of the Coney Island treatment plant are located at different heights, in a flooding event with a particular flood depth, some parts of WWTP fail and others may work as before. Table 8 shows the proximity of different unit operations from the ground level of Coney Island WWTP (NYCDEP 2013) and the assigned percentage of treatment share.

Although the numbers presented in Table 8 may not be an indicator of the actual percentage of the plant's operation under different flooding depth, they are estimated based on the information published by NYC-DEP, consultation with experts, and engineering judgement for the purpose of developing the methodology based on the AHP method to show the importance of the units. Even though the percentage of treatment is a reflection of the importance of each unit, it should be noted that the failure of one component may yield to the failure of the entire system. As an example, at the flood depth of 2.743 m (9 ft), most of the system's components below that depth fail because of the way different unit operations are positioned, but it can still partially operate at 30.7% of its capacity. The calculated CSO volumes in these scenarios are shown in Table 9.

SUMMARY AND CONCLUSION

Combined sewer treatment systems in coastal areas have a significant role in urban systems' serviceability and are vulnerable to heavy rain and flooding events. This vulnerability is intensified at the time of coastal storms. During an intense flood, runoff volume may exceed the capacity of a WWTP causing overflows and sewage to bypass into natural water bodies. This leads to different impacts such as environmental predicaments of significant proportions. In this study, a framework is proposed to quantify the impacts of CSOs in four different criteria such as human health, economics, social, and the environment by defining 22 different sub-criteria for each aspect. Because of the low resiliency, a high volume of CSO, and high damages during Hurricane Sandy, Coney Island WWTP is used as the case study. The AHP method was used for weighting the criteria and sub-criteria based on expert's

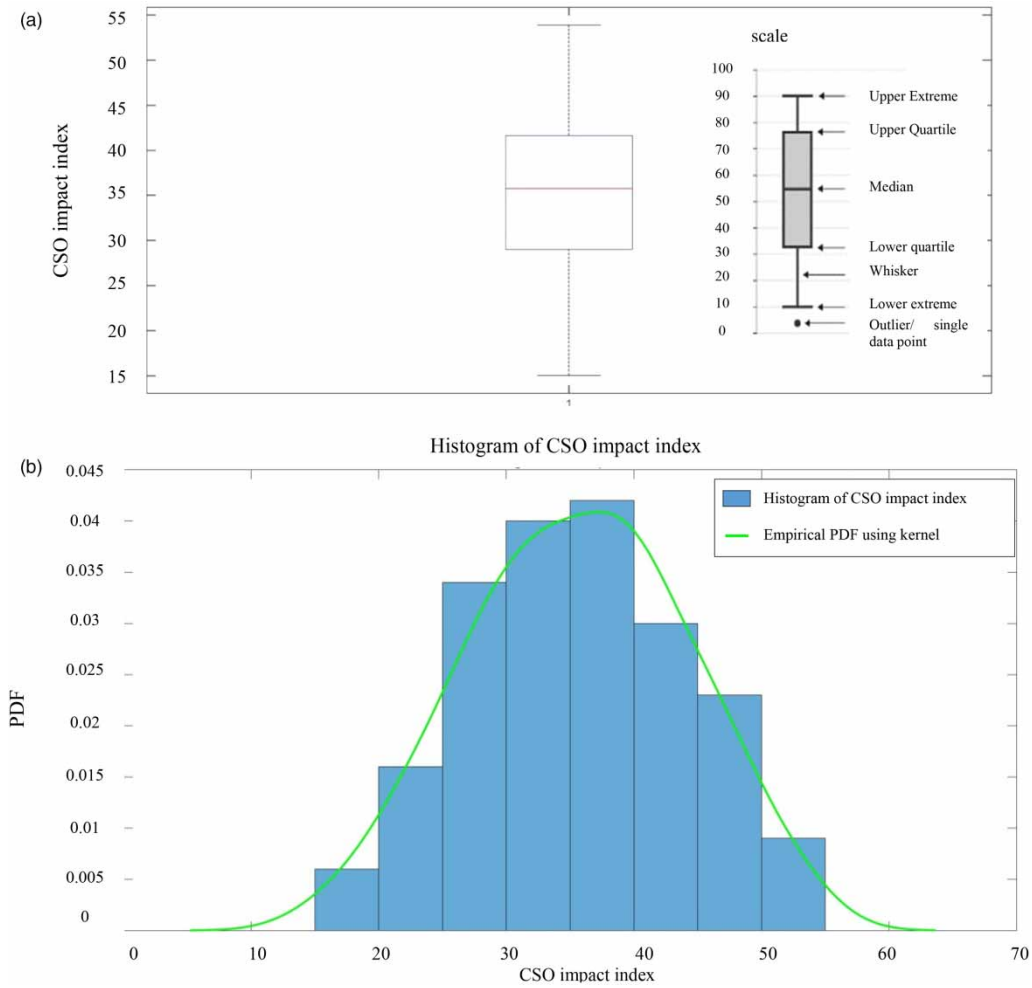

Figure 6 | (a) Range of CSO impact variation and (b) histogram of CSO impact index and empirical PDF using kernel.

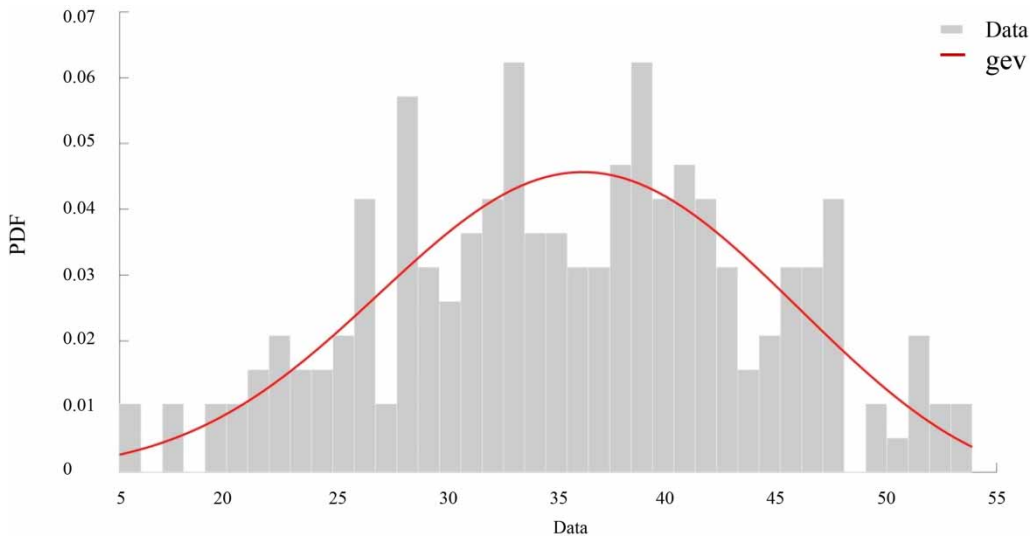

Figure 7 | PDF of gev distribution.

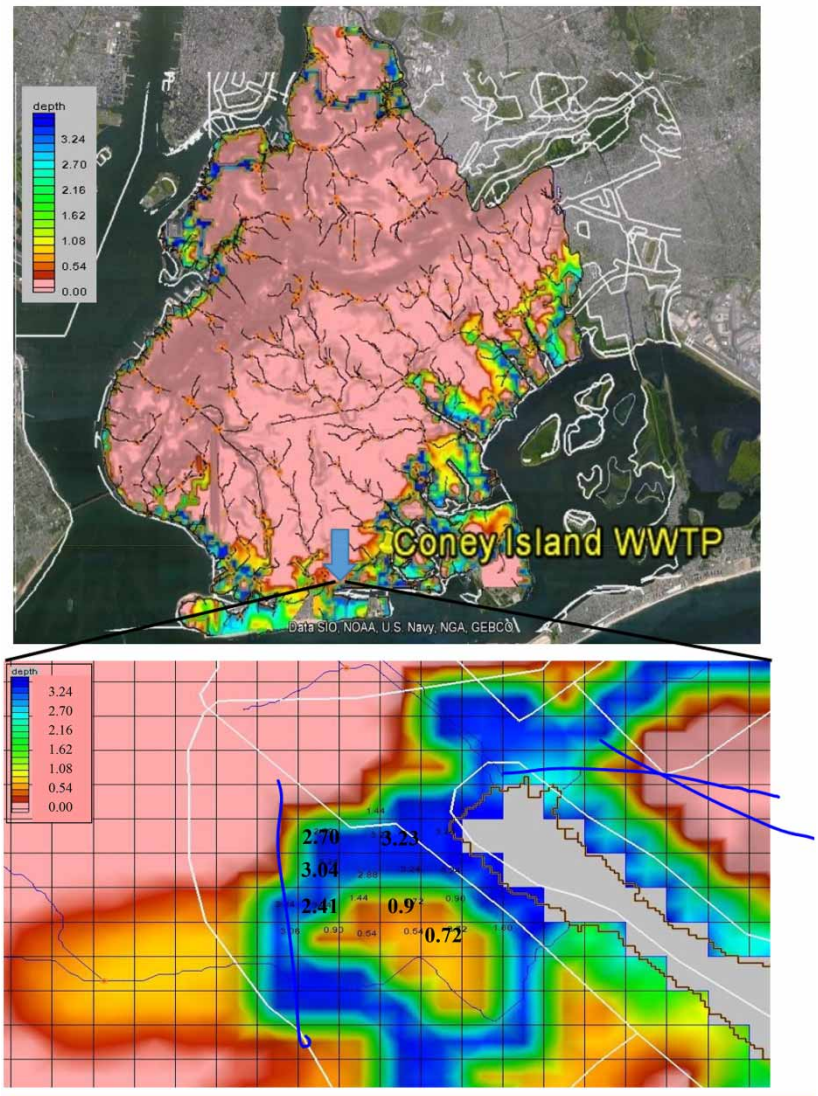

Figure 8 | Inundation depth in different parts of the drainage area affecting Coney Island WWTP after Superstorm Sandy and inundation depth for each cell.

opinions by using online questionnaires. Considering the actual, maximum, and minimum values of the sub-criteria, the PROMETHEE and fuzzy TOPSIS were used to quantify the impacts of CSO. The PROMETHEE result with an account of 0.475 shows the average impact condition after Superstorm Sandy in NYC. The results show that the environmental sub-criteria such as volume and depth have the most severe impacts. Then, five important sub-criteria with an uncertain nature were selected for further analysis, based on the Monte Carlo simulation, using PROMETHEE methods. Also, the results of sensitivity analysis indicate that TSS, BOD, and DO have the highest impact on CSO output.

For floodplain delineation, determining flood depth and runoff volume, the GSSHA model was used considering the Hurricane Sandy information. The results indicate that flood inundation depth at the most critical point was 3.78 m, and the maximum flooded inundation at the Coney Island WWTP location was estimated at 3.24 m. To evaluate changes in the CSOs volume affecting the environmental conditions, the volume of runoff is estimated using GSSHA as 763 million gallons. The produced wastewater in the drainage area of Coney Island WWTP was 60 million gallons per day. Finally, according to the WWTP response to flooding, three scenarios of the total, partial,

Table 8 | Percentage of system's operation at different inundation depths after Superstorm Sandy

Proximity of units/inundation depths (ft)	Different units of Coney Island treatment plant	Percentage share of treatment (%)	Cumulative not operating (%)
10.5	Primary screening building	3.4	0
10	Main building	7.1	3.4
	Pump and power building	10.1	10.5
	Odour control building	4.5	20.6
	Tunnel B	5.6	25.1
9	Grit building	3.4	30.7
	Plant maintenance building	5.6	34.1
	Thickener building	5.5	39.7
	Main electrical substation	7.9	45.2
	Activated sludge system	8.9	53.1
	Coloration system	8.7	62
8	Old power house	5.6	70.7
	Distributed power	7.9	76.3
	Sludge storage building	5.7	84.2
	Digester	5.5	89.9
	Tunnel A	4.6	95.4

Table 9 | CSO volume for different flood scenarios

Scenario	WWTP operational state (%)	Runoff volume (MCM/MG)	The volume of wastewater produced (MCM/MG)	Wastewater treatment capacity (MCMD/MGD)	Volume of CSO (MCM/MG)
1 (full operation)	100	2.89 MCM (763 MG)	0.28 MCM (60 MG)	0.48 MCMD (110 MGD)	2.9 MCM (663 MG[a])
2 (total failure)	0			0	3.8 MCM (883 MG)
3 (partial failure)	70.7			0.34 MCMD (77.77 MGD)	3.2 MCM (727.46 MG)
	30.7			0.14 MCMD (33.77 MGD)	3.5 MCM (815.46 MG)
	3.4			0.16 MCMD (3.74 MGD)	3.8 MCM (876.2 MG)

Note: MG, million gallons; mgd, million gallons per day.

[a]Superstorm Sandy duration was 2 days, so the volume of wastewater and treatment capacity are multiplied by 2 and then used in Equation (8).

and no failures were defined and the volumes of CSO were estimated in different scenarios. Not accessing to wastewater network of NYC and lack of data in the location of CSO's outfalls was the major limitation of this study. This topic would provide a worst-case flood scenario that could affect wastewater infrastructure. The results show that the proposed approach can be used to quantify the CSO impacts and also to identify which regions have the most exposure to prioritize investments and for better cost assessment of preparation, remediation, and recovery during floods. This will promote more effective use of funding opportunities for better future planning of wastewater infrastructure. It gives benefit points to operators of WWTPs to manage the CSOs during storms. For future investigation, researchers can develop uncertainty of hydrological models in flood estimation, and/or develop methods to ensure recovery and quick return of the treatment plant to its required function. Moreover, one can evaluate the vulnerability of the case study WWTP to the storm-driven waves in addition to the CSOs as a future study.

DATA AVAILABILITY STATEMENT

All relevant data are included in the paper or its Supplementary Information.

REFERENCES

Al-Ani, R. R. A. & Al-Obaidi, B. H. K. 2019 Prediction of sediment accumulation model for trunk sewer using multiple linear

regression and neural network techniques. *Civil Engineering Journal* **5** (1), 82–92. doi:10.28991/cej-2019-03091227.

Bae, H. K. 2020 The effect of combined sewer overflows on river's water quality. *Membrane Water Treatment* **11** (1), 49–57. https://doi.org/10.12989/mwt.2020.11.1.049.

Boët, P., Duvoux, B., Allardi, J. & Belliard, J. 1994 The influence of summer stormwater on the fish community of Seine River below the urban area of Paris (en). *La Houille Blanche* **1–2**, 141–147. doi:10.1051/lhb/1994020.

Bowman, M. J., Colle, B. A., Buonaiuto, F., Wilson, R. E., Flood, R., Hunter, R. & Hill, D. 2008 New York City's vulnerability to coastal flooding. *Bulletin of the American Meteorological Society* **89** (6), 829–841. https://doi.org/10.1175/2007BAMS2401.1.

Burgan, H. I. & Icaga, Y. 2019 Flood analysis using adaptive hydraulics (AdH) model in Akarcay Basin. *Teknik Dergi* **30** (2), 9029–9051. https://doi.org/10.18400/tekderg.416067.

De Almeida, B. A. & Mostafavi, A. 2016 Resilience of infrastructure systems to sea-level rise in coastal areas: impacts, adaptation measures, and implementation challenges. *Sustainability* **8** (12), 1115–1142. https://doi.org/10.3390/su8111115.

Downer, C. & Ogden, F. 2004 GSSHA: Model to simulate diverse stream flow producing processes. *Journal of Hydrologic Engineering* **9** (3), 161–174. https://doi.org/10.1061/(ASCE)1084-0699(2004)9:3(161).

Fotovatikhah, F., Herrera, M., Shamshirband, S., Chau, K. W., Faizollahzadeh Ardabili, S. & Piran, M. J. 2018 Survey of computational intelligence as basis to big flood management: challenges, research directions and future work. *Engineering Applications of Computational Fluid Mechanics* **12** (1), 411–437. https://doi.org/10.1080/19942060.2018.1448896.

Friedrich, E. & Kretzinger, D. 2012 Vulnerability of wastewater infrastructure of coastal cities to sea level rise: a South African case study. *Water South Africa* **38** (5), 755–764. doi:10.4314/wsa.v38i5.15.

Gandhi, R. 2013 *Treatment of Combined Sewer Overflows Using Ferrate (VI)*. Chemical and Biochemical Engineering, The School of Graduate and Postdoctoral Studies, The University of Western Ontario London, Master of Engineering Science, Ontario, Canada. https://doi.org/10.2175/106143014X14062131178475.

Golian, S., Saghafian, B. & Farokhnia, A. 2012 Copula-based interpretation of continuous rainfall–runoff simulations of a watershed in northern Iran. *Canadian Journal of Earth Sciences* **49** (5), 681–691. https://doi.org/10.1139/e2012-011.

Gornitz, V., Couch, S. & Hartig, E. K. 2002 Impacts of sea level rise in the New York City metropolitan area. *Global and Planetary Changes* **32**, 61–88. https://doi.org/10.1016/S0921-8181(01)00150-3.

Harremoes, P. 1982 Immediate and delayed oxygen depletion in rivers. *Water Research* **16**, 1093–1098. https://doi.org/10.1016/0043-1354(82)90124-5.

Haq, M., Akhtar, M., Muhammad, S., Paras, S. & Rahmatullah, J. 2012 Techniques of remote sensing and GIS for flood monitoring and damage assessment: a case study of Sindh province, Pakistan. *The Egyptian Journal of Remote Sensing and Space Science* **15** (2), 135–141. https://doi.org/10.1016/j.ejrs.2012.07.002.

Holeton, C., Chambers, P. A. & Grace, L. 2011 Wastewater release and its impacts on Canadian waters. *Canadian Journal of Fisheries and Aquatic Sciences* **68** (10), 1836–1859. https://doi.org/10.1139/f2011-096.

Horritt, M. S. & Bates, P. D. 2001 Predicting floodplain inundation: raster-based modelling versus the finite-element approach. *Hydrological Processes* **15**, 825–842. https://doi.org/10.1002/hyp.188.

House, M. A., Ellis, J. B., Herricks, E. E., Hvitved-Jacobsen, T., Seager, J., Lijklema, L. & Clifforde, I. T. 1993 Urban drainage-impacts on receiving water quality. *Water Science and Technology* **27** (12), 117. https://doi.org/10.2166/wst.1993.0293.

Hummel, M. A., Berry, M. S. & Stacey, M. T. 2018 Sea level rise impacts on wastewater treatment systems along the U.S. coasts. *Earth's Future* **6**, 622–633. https://doi.org/10.1002/2017EF000805.

Hwang, C. L. & Yoon, K. 1981 Methods for multiple attribute decision making. In: *Multiple Attribute Decision Making*. Springer, Berlin, Heidelberg, pp. 58–191. https://doi.org/10.1007/978-3-642-48318-9_3.

Karamouz, M., Abbasi, H., Fereshtehpour, M. & Bidhendi, G. R. N. 2015 Multicriteria Evaluation of Combine Sewer Overflow Impacts in Coastal Cities. In: *EWRA Conference*.

Karamouz, M. & Abbasi, H. 2016 Determination of CSO volume for impact assessments under extreme flooding conditions: a case study. In: *World Environmental and Water Resources Congress*, 2016, pp. 162–170. https://doi.org/10.1061/9780784479858.018.

Kaya, C. M., Tayfur, G. & Gungor, O. 2019 Predicting flood plain inundation for natural channels having no upstream gauged stations. *Journal of Water and Climate Change* **10** (2), 360–372.

Kenward, A., Yawitz, D. & Raja, U. 2013 *Sewage Overflows from Hurricane Sandy*. Climate Central, Princeton, NJ.

Keum, H. J., Han, K. Y. & Kim, H. I. 2020 Real-time flood disaster prediction system by applying machine learning technique. *KSCE Journal of Civil Engineering* **24** (9), 2835–2848. https://doi.org/10.1007/s12205-020-1677-7.

Kokoszka, M. 2013 *Reassessing Vulnerability: Using a Holistic Approach and Critical Infrastructure to Examine Flooding in New York City*. Project Report, Polytechnic Institute of New York University, New York.

Madoux-Humery, A. S., Dorner, S., Sauvé, S., Aboulfadl, K., Galarneau, M., Servais, P. & Prévost, M. 2013 Temporal variability of combined sewer overflow contaminants: evaluation of wastewater micropollutants as tracers of fecal contamination. *Water Research* **47** (13), 4370–4382. https://doi.org/10.1016/j.watres.2013.04.030.

Maidment, D. R. 1993 *Handbook of Hydrology* (Vol. 9780070, p. 397323). McGraw-Hill, New York. https://doi.org/10.1061/9780784401385.

Mirra, R., Ribarov, C., Valchev, D. & Ribarova, I. 2020 Towards energy efficient onsite wastewater treatment. *Civil Engineering Journal* **6** (7), 1218–1226. doi:10.28991/cej-2020-03091542.

Morais, D. C. & de Almeida, A. T. 2007 Group decision-making for leakage management 186 strategy of water network. *Resources, Conservation and Recycling* **52** (2), 441–459. https://doi.org/10.1016/j.resconrec.2007.06.008.

Mosavi, A., Ozturk, P. & Chau, K. W. 2018 Flood prediction using machine learning models: literature review. *Water* **10** (11), 1536. https://doi.org/10.3390/w10111536.

Moya, V., Popescu, I., Solomatine, D. P. & Bociort, L. 2013 Cloud and cluster computing in uncertainty analysis of integrated flood models. *Journal of Hydroinformatics* **15** (1), 55–70. https://doi.org/10.2166/hydro.2012.017.

National Oceanic and Atmospheric Administration (NOAA) 2012 Available from: https://www.ncdc.noaa.gov/cdo-web/datasets/GHCND/stations/GHCND:USW00094728/detail.

New York City (NYC) environmental protection 2012a *New York City 2012 Drinking Water Supply and Quality Report*. Available from: https://www1.nyc.gov/assets/dep/downloads/pdf/water/drinking-water/drinking-water-supply-quality-report/2019-drinking-water-supply-quality-report.pdf.

New York City (NYC) environmental protection 2012b Available from: https://www1.nyc.gov/site/dep/water/history-of-drought-water-consumption.page.

NYCDEP 2013 *NYC Wastewater Resiliency Plan', Climate Risk Assessment and Adaptation 221 Study, Chapter 2: Wastewater Treatment Plant*. Department of environmental protection, 222, New York City. https://doi.org/10.1061/9780784478745.021.

Passerat, J., Ouattara, N. K., Mouchel, J. M., Rocher, V. & Servais, P. 2011 Impact of an intense combined sewer overflow event on the microbiological water quality of the Seine River. *Water Research* **45** (2), 893–903. https://doi.org/10.1016/j.watres.2010.09.024.

Saaty, T. 1977 A scaling method for priorities in hierarchical structures. *Mathematical Psychology* **15** (3), 234–281. https://doi.org/10.1016/0022-2496(77)90033-5.

Schroeder, K., Riechel, M., Matzinger, A., Rouault, P., Sonnenberg, H., Pawlowsky-Reusing, E. & Gnirss, R. 2011 Evaluation of effectiveness of combined sewer overflow measures by operational data. *Water Science and Technology* **63** (2), 325–330. https://doi.org/10.2166/wst.2011.058.

Semadeni-Davies, A., Hernebring, C., Svensson, G. & Gustafsson, L.-G. 2008 The impacts of climate change and urbanisation on drainage in Helsingborg, Sweden: combined sewer system. *Journal of Hydrology* **350** (1–2), 100–113. https://doi.org/10.1016/j.jhydrol.2007.05.028.

Sobol, I. M. 2001 Global sensitivity indices for nonlinear mathematical models and their Monte Carlo estimates. *Mathematics and Computers in Simulation* **55** (1–3), 271–280. https://doi.org/10.1016/S0378-4754(00)00270-6.

Tang, Y., Reed, P., Wagener, T. & Van Werkhoven, K. 2007 Comparing sensitivity analysis methods to advance lumped watershed model identification and evaluation. *Hydrology and Earth System Sciences* **11** (2), 793–817. https://doi.org/10.5194/hess-11-793-2007.

Taormina, R. & Chau, K. W. 2015 ANN-based interval forecasting of streamflow discharges using the LUBE method and MOFIPS. *Engineering Applications of Artificial Intelligence* **45**, 429–440. https://doi.org/10.1016/j.engappai.2015.07.019.

Toda, K., Inoue, K., Nishikori, T. & Nakagawa, Y. 2005 Inundation analysis by heavy rainfall in urban area considering branch sewer effect. In *Proceedings of the International Conference on Monitoring, Prediction and Mitigation of Water Related Disasters*, Kyoto, Japan, pp. 137–141.

Tung, Y. K. & Yen, B. C. 2006 *Hydrosystems Engineering, Uncertainty Analysis*. McGraw-Hill, New York, NY, USA.

United states Environmental Protection Agency (UEPA) 2001 *Report to Congress Implementation and Enforcement of the Combined Sewer Overflow Control Policy, Office of Water (4203), Washington D.C. 20460, December*.

United states Environmental Protection Agency (UEPA) 2004 *Report to Congress: Impacts and Control of CSOs and SSOs', Office of Water (4203), Washington D.C. 20460, August*.

United states Environmental Protection Agency (UEPA) 2013 *A Primer for Remedial Project Managers on Water Quality Standards and the Regulation of Combined Sewage Overflows Under the Clean Water Act, Office of Water (4203), Washington D.C. 20460, December*.

United states Environmental Protection Agency (UEPA) 2017 *What are Combined Sewer Overflows (CSOs)?* Available from: https://www3.epa.gov/region1/eco/uep/cso.html.

Vincke, J. P. & Brans, P. 1985 A preference ranking organization method. The PROMETHEE method for MCDM. *Management Science* **31** (6), 647–656. https://doi.org/10.1287/mnsc.31.6.647.

Walsh, C. J., Fletcher, T. D. & Ladson, A. R. 2005 Stream restoration in urban catchments through redesigning stormwater systems: looking to the catchment to save the stream. *Journal of the North American Benthological Society* **24** (3), 690–705. https://doi.org/10.1899/04-020.1.

Wu, C. L. & Chau, K. W. 2013 Prediction of rainfall time series using modular soft computing methods. *Engineering Applications of Artificial Intelligence* **26** (3), 997–1007. https://doi.org/10.1016/j.engappai.2012.05.023.

Zadeh, L. A. 1996 Fuzzy sets. In *Fuzzy sets, fuzzy logic, and fuzzy systems: selected papers by Lotfi A Zadeh* (G. J. Klir & B. Yuan, eds). WSPC, pp. 394–432.

Zeynolabedin, A., Ghiassi, R. & Dolatshahi Pirooz, M. 2020 Seawater intrusion vulnerability evaluation and prediction: a case study of Qeshm Island, Iran. *Journal of Water and Climate Change*. https://doi.org/10.2166/wcc.2020.220.

Zheng, N., Tachikawa, Y. & Takara, K. 2008 A distributed flood inundation model integrating with rainfall-runoff processes using GIS and remote sensing data. *The International Archives of the Photogrammetry, Remote Sensing and Spatial Information Sciences* **37** (4), 1513–1518.

First received 18 November 2020; accepted in revised form 9 March 2021. Available online 22 March 2021